Ticks and Tick-borne Diseases 10 (2019) 1018–1027

Contents lists available at ScienceDirect

Ticks and Tick-borne Diseases

journal homepage: www.elsevier.com/locate/ttbdis

Original article

4-NBT, a specific inhibitor of *Babesia microti* thioredoxin reductase, affects parasite biochemistry and proteomic properties

Yanzhen Zhao, Jingwei Huang, Jie Cao, Yongzhi Zhou, Haiyan Gong, Houshuang Zhang, Jinlin Zhou*

Key Laboratory of Animal Parasitology of Ministry of Agriculture, Shanghai Veterinary Research Institute, Chinese Academy of Agricultural Sciences, Shanghai 200241, China

ARTICLE INFO

Keywords:
Babesia microti
Thioredoxin reductase
4-NBT

ABSTRACT

Babesia microti is an emerging zoonotic pathogen that is transmitted by ticks and parasites and propagates in mammalian erythrocytes. Thioredoxin reductase (TrxR) plays a crucial role in *B. microti* survival by maintaining cellular redox homeostasis. In the present study, 4-nitro-2,1,3-benzothiadiazole (4-NBT) was selected as a specific *B. microti* TrxR inhibitor by comparing rat and parasite TrxR inhibition levels. Reactive oxygen species (ROS) levels were evaluated using flow cytometry, and in *B. microti* treated with 4-NBT, ROS levels increased with increasing inhibitor concentration. Furthermore, the inhibitor treatment increased lipid peroxidation and protein carbonyl levels, thus indicating a state of oxidative stress. While *B. microti* treated with 4-NBT appeared to lose the ability to multiply in mice, the fastigium of parasitemia between the treated and control groups was comparable. Furthermore, a TUNEL assay showed that 4-NBT induces apoptosis in *B. microti*. Proteomic analysis of *B. microti* treated with 4-NBT detected 960 proteins. Label-free quantitative proteomic analysis identified 118 proteins that were significantly up-regulated and 37 that were significantly down-regulated in the treatment group relative to the control. Of the differential proteins, proteasome and ribosomal subunit expression was up-regulated, thus suggesting that redundant proteins may be damaged by oxidation and waiting for degradation, while proteins for subsistence are waiting for *de novo* synthesis. Moreover, the findings obtained herein suggest that the DNA and lipids were also damaged and awaiting synthesis or repair. In conclusion, TrxR dysfunction in *B. microti* results in the breakdown of redox homeostasis and promotes apoptosis.

1. Introduction

Babesia microti is an intraerythrocytic protozoan that causes emerging and zoonotic babesiosis. To date, human *B. microti* infections have been reported in many countries, including the United States, Australia, Germany, Japan, and China (Vannier and Krause, 2012). This spread means that the risk of babesiosis is increasing with time, and it now has become a global threat to public health. The clinical symptoms of babesiosis are generally mild in immunocompetent patients but acute and serious in immunocompromised patients (Vannier et al., 2008). Currently, the most effective treatment is to utilize a combination of the drugs atovaquone and azithromycin, but these may cause adverse effects, such as fever, emesis, dizziness, arrhythmia, or anaphylaxis (Krause et al., 2000). Furthermore, with the presence of antibiotic resistance, it is imperative and urgent to identify new therapeutic targets that can aid in the development of a new potent drug to mitigate *B. microti*.

B. microti parasitizes mammalian erythrocytes due to their high iron concentrations and hyperoxic environment (Müller, 2010). Since *B. microti* is sensitive to oxidative stress, it neutralizes the toxic effects of ROS and reactive nitrogen species (RNS) (Kehr et al., 2010). In *B. microti*, the glutathione S-transferase gene, and subsequent glutathione reduction, has yet to been identified, thus suggesting that the glutathione and antioxidant systems are underdeveloped when compared to an organism like *Plasmodium falciparum* (Cornillot et al., 2012). Therefore, the thioredoxin system becomes very valuable, even critical, to survival in erythrocytes. The main function of the thioredoxin system is to regulate cellular redox status by eliminating ROS and repairing any peroxidation damage (Kavishe et al., 2017). The system is composed of several thioredoxins, thioredoxin reductase (TrxR), and NADPH. TrxR, a key enzyme of this system, not only reduces Trx but also transfers electrons to low molecular weight compounds (Jortzik and Becker, 2012). Previously, our laboratory identified a unique TrxR in *B. microti* with two distinct active centers that facilitate the electron transfer from

* Corresponding author.
E-mail address: jinlinzhou@shvri.ac.cn (J. Zhou).

https://doi.org/10.1016/j.ttbdis.2019.05.004
Received 30 January 2019; Received in revised form 21 April 2019; Accepted 17 May 2019
Available online 22 May 2019
1877-959X/

NADPH to a substrate *via* a disulfide FAD domain, and a C-terminal redox center consisting of two cysteines separated by four amino acids (Zhao et al., 2016). These features distinguish this TrxR from mammalian TrxRs, which contain a cysteine-selenocysteine motif (Andricopulo et al., 2006). In *P. falciparum*, TrxR is necessary during the intraerythrocytic stages (Krnajski et al., 2002), and TrxR inhibition using Auranofin has been shown to inhibit *P. falciparum* growth *in vitro* (Sannella et al., 2008). Thus, TrxR is a potential drug target in the treatment of *Babesia*.

Herein, TrxR mechanisms and how they contribute to *B. microti* survival were examined. Red blood cells (RBCs) were infected with *B. microti in vitro* and treated with 4-NBT, a specific *B. microti* TrxR inhibitor, and differences in protein expression in the parasite were analyzed using a label-free quantitative proteomic approach.

2. Material and methods

2.1. Ethics statement

All of the animal experimentation and protocols were approved by the Institutional Animal Care and Use Committee of the Shanghai Veterinary Research Institute (IACUC approve number shvri-mo-0054) and authorized by the Animal Ethical Committee of Shanghai Veterinary Research Institute. This study was compliant with ARRIVE guidelines and EU Directive 2010/63/EU for animal experiments.

2.2. B. microti cultured in vitro

B. microti was obtained from the American Type Culture Collection (ATCC^{R} PRA-99$^{™}$) and cultured *in vivo* using the serial passage in KM mice as previously described (Zhang et al., 2016). For *in vitro* culturing, infected blood was collected as described previously and washed three times with RPMI and HEPES and centrifuged. The obtained erythrocytes were then suspended in *B. microti* complete culture medium (BCM), which comprised RPMI 1640 (Gibco, Carlsbad, CA, USA), 25 mM HEPES (Gibco, Carlsbad, CA, USA), 0.1% Penicillin-Streptomyocin (Gibco, Carlsbad, CA, USA), 3.5X HT supplement (Gibco, Carlsbad, CA, USA), and 0.5% bovine serum albumin (BSA; Equitechbio, Kerrville, TX, USA) (Trager and Jensen, 2005). Parasites were maintained utilizing the microaerophilous stationary phase (MASP) culturing method as previously described, with slight modifications (Erp et al., 1980; Levy and Ristic, 1980; Taylor and Baker, 1987). Briefly, the erythrocytes were diluted with BCM to obtain 2% hematocrit, and the liquid-column height was maintained at 0.62 cm. The cultures were then placed in a cell incubator at 37 °C, with 5% CO_2, and the medium was changed daily.

2.3. Selecting a TrxR inhibitor for B. microti

Four effective compounds have been reported to inhibit TrxR, namely, Auranofin, CDNB (1-chloro 2,4-dinitrobenzene), 4-NBT (4-nitro-2,1,3-benzothiadiazole), and 2,4-DNPS (2,4-dinitrophenyl sulfide) (Andricopulo et al., 2006). Each compound was tested for its ability to inhibit *B. microti* TrxR (*Bm*TrxR) and/or rat TrxR (RTrxR) at different concentrations, with TrxR activity levels determined using a Thioredoxin Reductase Assay Kit (Sigma-Aldrich, St. Louis, MO, USA) with slight modifications. Plots were then constructed to determine associations between drug concentration and TrxR inhibition rate, with IC50 values also determined.

2.4. Culturing parasites in vitro with 4-NBT

Parasites were maintained as described above. After two days, parasite-infected red blood cells (IRBCs) at 10% parasitemia were incubated in BCM containing 4-NBT at a concentration of 25, 50, or 100 μM for 12 h at 37 °C and 5% CO_2, with the negative control sample only treated with DMSO. After 12 h, the IRBCs were pelleted and washed three times in PBS and lysed by adding 20x packed cell volume of 0.05% saponin in PBS and allowed to sit on ice for less than 30 min. Resulting lysates were then washed in PBS until turning white. The precipitates were suspended in PBS supplemented with protease inhibitor (Cell Biolabs, San Diego, CA, USA), and then sonicated on ice for about 2 min (1 s on and 1 s off intervals) at a 10% amplitude (Bullard et al., 2015). The samples were then centrifuged at 10,000 rpm for 10 min at 4 °C, and the supernatants containing *B. microti* were extracted.

2.5. SYBR® Green I parasite growth assay

In previous studies, SYBR® Green I parasite growth assay has been utilized in *Plasmodium* to determine the relationship between drug susceptibility and growth (Smilkstein et al., 2004). Assays were conducted in a 96-well plate in a total volume of 200 μl [199 μl BCM with 2% haematocrit at 5% parasitemia and 1 μl treatment (4-NBT or DMSO)], with test samples treated with 4-NBT (25, 50, or 100 μM) dissolved in DMSO and the negative control treated with only DMSO. After 12 h, 100 μl from each culture was transferred to a new blank plate, and 100 μl of RBC lysis buffer (20 mM Tris base, 5 mM EDTA, 0.0008% saponin, 0.08% Triton X-100, pH 7.5 with 0.2 μl SYBR® Green I/ml of lysis buffer) was added to each well. Plates were incubated in the dark for 30 min, and then fluorescence levels were quantified (excitation 485 nm, emission 535 nm).

2.6. How 4-NBT affects parasite vitality

To assess the effect of 4-NBT on *B. microti* vitality and infectivity, erythrocytes were collected from mice infected with *B. microti*, with a parasitemia up to 40%, and cultured *in vitro* for two days prior to 4-NBT or DMSO (control) treatment as described above. Five-week-old female BALB/C mice were randomly divided into five groups of five as follows: DMSO (control), 25 μM 4-NBT group, 50 μM 4-NBT group, 100 μM 4-NBT group, and healthy erythrocytes (negative control), with each group inoculated intraperitoneally with 1×10^8 corresponding erythrocytes. The percentage of parasitemia was then determined using flow cytometry.

2.7. Hemolytic activity following 4-NBT treatment

To evaluate 4-NBT cytotoxicity, the degree of hemolysis was determined following treatment (Nilsson Bark et al., 2018). The same number of infected erythrocytes were treated with either DMSO (control) or 25, 50, or 100 μM of 4-NBT as described above. As a positive lysis control, erythrocytes were incubated with 0.4% Triton-X 100, while the negative control was only incubated with BCM. After 12 h, samples were centrifuged and the supernatants were collected. The amount of released hemoglobin (Hb) was measured at $OD_{415\ nm}$, and the degree of lysis per sample was calculated as follows: lysis (test sample) = [test sample ($OD_{415\ nm}$) – blank ($OD_{415\ nm}$)] / [positive lysis control ($OD_{415\ nm}$) – blank ($OD_{415\ nm}$)], and presented as a percentage.

2.8. Reactive oxygen species levels following 4-NBT

ROS production was determined by employing a CellROX™ Deep Red Flow Cytometry Assay Kit (Thermo Fischer Scientific, Waltham, MA, USA). IRBCs were treated with various 4-NBT concentrations as described above. Cells were then stained with 1 μM CellROX® Deep Red reagent for 60 min at 37 °C, and then with 1x SYBR® Green (Sigma) for 30 min at room temperature.

2.9. TrxR activity in the presence of 4-NBT

The total protein concentrations of *B. microti* extracts were

measured using a Pierce™ BCA Protein Assay Kit (Thermo Fischer Scientific), with the samples derived as described above. TrxR activity was measured by adding DTNB [5,5′ - dithiobis (2-nitrobenzoic) acid] and then by measuring differences in sample concentrations at $OD_{412\ nm}$ for 5 h at 25 °C.

2.10. Lipid peroxidation levels with 4-NBT

Malondialdehyde (MDA), the end product of lipid peroxidation, was detected with a Lipid Peroxidation (MDA) Assay Kit (Sigma-Aldrich) according to the manufacturer's instructions. MDA-TBA (thiobarbituric acid) adducts form when the sample MDA reacts with the TBA and is detected spectrophotometrically at $OD_{532\ nm}$ to enable MDA quantification.

2.11. Protein carbonyl (PC) content levels with 4-NBT treatment

Protein carbonylation was detected using a Protein Carbonyl Content Assay Kit (Sigma-Aldrich) according to the manufacturer's instructions. Carbonyl content was quantified based on the derivatization of protein carbonyl groups in the presence of 2,4-dinitrophenylhydrazine (DNPH), which subsequently leads to the formation of a stable dinitrophenyl (DNP) hydrazone adduct that can be detected spectrophotometrically at $OD_{375\ nm}$.

2.12. TUNEL apoptosis assay

Erythrocytes infected with *B. microti* were treated with DMSO or 50 μM of 4-NBT as described above. Blood smears were prepared after collecting and washing the cells. The cells were fixed using methanol and acetone at a scale of 1:1. To detect apoptotic DNA fragments, a terminal deoxynucleotidyl transferase dUTP nick-end labeling (TUNEL) assay was performed by employing an *In Situ* Cell Death Detection kit (Roche Diagnostics, Mannheim, Germany), and smears were stained according to the manufacturer's protocols. In brief, the *B. microti* nuclei were stained blue using 4′,6′-diamidino-2-phenylindole (DAPI) (Thermo Scientific, Waltham, MA, USA), and apoptotic parasites were stained green using the TUNEL working buffer. Coverslips were mounted using Fluoromount Aqueous Mounting Media (Sigma-Aldrich, St. Louis, MO, USA), and slides were examined using a confocal laser-scanning microscope (Zeiss LSM 880, Oberkochen, Germany). The same parameters were used for both the experimental and control groups.

2.13. Label-free quantitative proteomic method

2.13.1. Protein extraction

To identify differential protein expression between *B. microti* incubated with 50 μM 4-NBT or DMSO, three biological replicates were examined for each and were tagged TNB1, TNB2, and TNB3 or TDM1, TDM2, and TDM3, respectively. After treatment, *B. microti* extracts were prepared as described above. The precipitates were suspended in SDT buffer (4% SDS, 100 mM Tris − HCl, 10 mM DTT, pH7.6). Each sample was sonicated and then boiled for 15 min. After centrifuged at 14,000 rpm for 40 min, the supernatant was quantified with BCA Protein Assay Kit (Bio-Rad. USA). 20 μg of proteins were analyzed by SDS-PAGE.

2.13.2. FASP Digestion and fractionation

Filter-aided sample preparation (FASP) were analyzed by the method described previously. 200 μg of protein for each sample were incorporated in SDT buffer (4% SDS, 100 mM DTT, 150 mM Tris − HCl, pH 8.0). The detergent, DTT and other low-molecular-weight components were removed using UA buffer (8 M urea, 150 mM Tris − HCl, pH 8.0) by repeated ultrafiltration (Microcon units,10KD). Then, 100 μL iodoacetamide (100 mM IAA in UA buffer) was added to block reduced cysteine residues, and the samples were incubated for 30 min in darkness. The filters were washed with 100 μL of UA buffer three times and then 100 μL of 25 mM NH_4HCO_3 buffer twice. Finally, the protein suspensions were digested with 4 μg of trypsin (Promega) in 40 μL of 25 mM NH_4HCO_3 buffer overnight at 37 °C, and the resulting peptides were collected as a filtrate. The peptides of each sample were desalted on C18 cartridges (Empore™ C18 SPE cartridges (standard density), bed I.D. 7 mm, volume, 3 ml, Sigma), concentrated by vacuum centrifugation and reconstituted in 40 μL of 0.1% (v/v) formic acid. The peptide content was estimated from the UV light spectral density at 280 nm using an extinction coefficient of 1.1 of 0.1% (g/L) solution that was calculated on the basis of the frequency of tryptophan and tyrosine in vertebrate proteins.(Wisniewski et al., 2009)。

Pierce high pH reversed-phase fractionation kit (Thermo scientific) was used to fractionate digest samples into 3 fractions by an increasing acetonitrile step-gradient elution according to instructions.

2.13.3. LC-MS/MS/ms

The mass spectrometry analysis was performed by Shanghai Applied Protein Technology Co. Ltd. Easy nLC liquid chromatograph (Thermo Scientific) was used to separate each sample. Buffer A consisted of 0.1% formic acid, while buffer B of 84% acetonitrile and 0.1% formic acid. The peptide mixture was loaded onto a reversed-phase trap column (Thermo Scientific Acclaim PepMap100, 100 μm*2 cm, nanoViper C18) connected to a C18 reversed-phase analytical column (Thermo Scientific Easy Column, 10 cm long, 75 μm inner diameter, 3 μm resin) in buffer A and separated with a linear gradient of buffer B at a flow rate of 300 nL/min controlled by IntelliFlow technology: 0–35% buffer B for 50 min, 35–100% buffer B for 5 min, and 100% buffer B for 5 min.

LC–MS/MS analysis was performed on a Q-Exactive mass spectrometer (Thermo Scientific) that was coupled to Easy nLC for 60 min. The mass spectrometer was operated in positive ion mode. MS data were acquired using a data-dependent top-10 method that dynamically chose the most abundant precursor ions from the survey scan (300–1800 m/z) for high-energy collisional dissociation (HCD) fragmentation. Automatic gain control target was set to 1e6, and maximum inject time to 50 ms. Dynamic exclusion duration was 60 s. Survey scans were acquired at a resolution of 70,000 at 200 m/z, the resolution of the HCD spectra was set to 17,500 at 200 m/z, and the isolation window was 2 m/z. The normalized collision energy was 30 eV, and the underfill ratio was defined as 0.1%.

The obtained MS data were analyzed using MaxQuant software version 1.5.3.17 (Max Planck Institute of Biochemistry, Martinsried, Germany) (Cox and Mann, 2008). The following parameters were set as shown in Table 1. What's more, the proteomics data were available *via* ProteomeXchange with identifier PXD013126.

Table 1
The relative parameters of MS analysis.

Item	Value
Enzyme	Trypsin
Max Missed Cleavages	2
Main search	6 ppm
First search	20 ppm
MS/MS Tolerance	20 ppm
Fixed modifications	Carbamidomethyl (C)
Variable modifications	Oxidation (M), Acetyl (Protein N-term)
Database	uniprot_*Babesia_microti*_3748_20180622 database
Database pattern	Reverse
Peptide FDR	< 0.01
Protein FDR	< 0.01
Time window (match between runs)	2 min
Protein Quantification	Razor and unique peptides were used for protein quantification
LFQ	True
LFQ min. ratio count	1

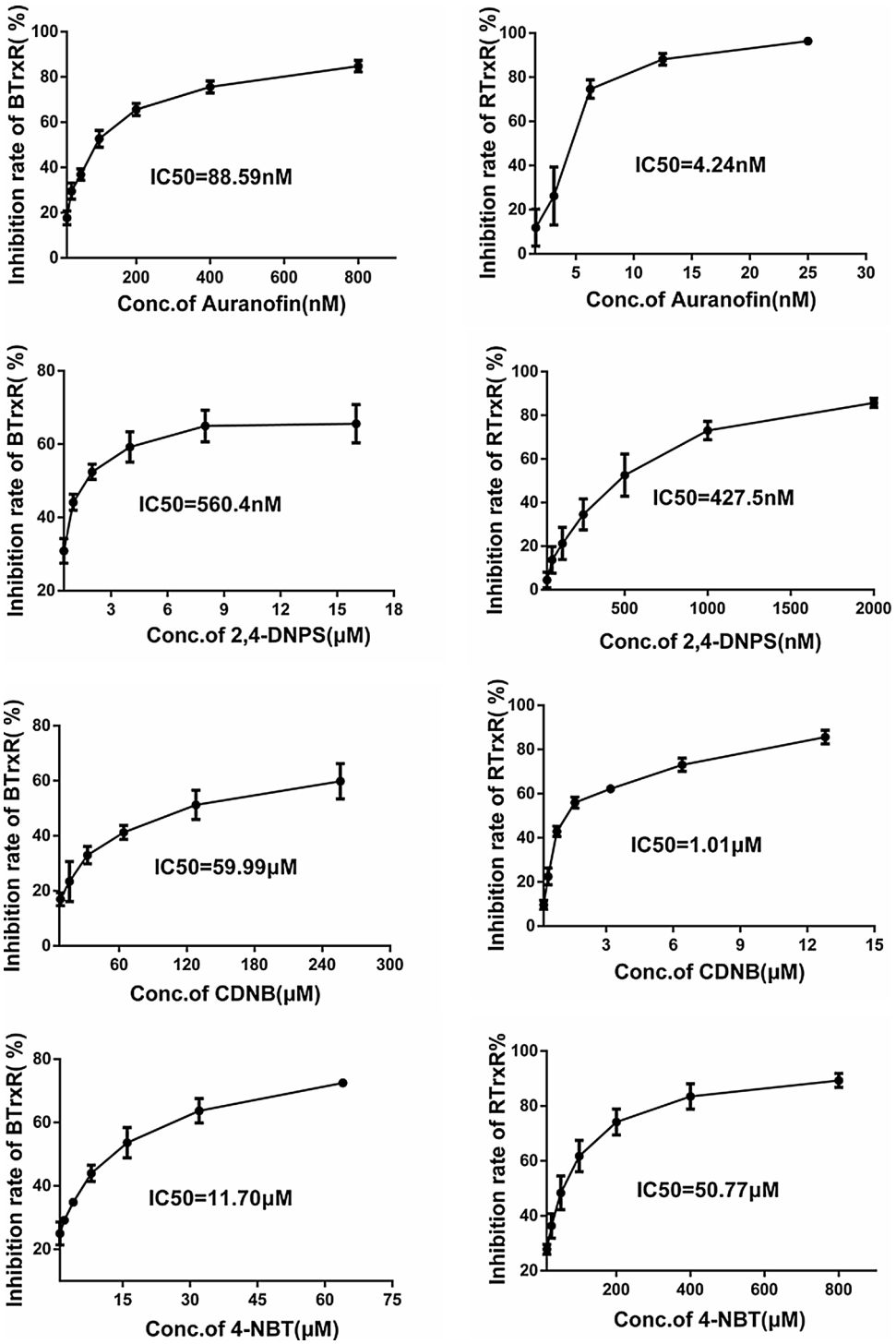

Fig. 1. Correlation curves between TrxR drug concentration and inhibition rate. Identifying the most selective *Bm*TrxR inhibitor out of Auranofin (A), 2,4-DNPS (B), CDNB (C), or 4-NBT (D) using the DTNB reduction method. Inhibitors were applied to both *Bm*TrxR (left) and RTrxR (right) samples at the designated IC50 values.

2.13.4. Bioinformatics analysis

Proteins were identified as differentially expressed if a fold-change > 2 and P-value < 0.05 were obtained and if the protein was identified in 2 or more of the replicates within a group while not detected in the other group. The identified differential proteins were then characterized using Gene Ontology (GO) in Blast2GO (version go_201504.obo; www.geneontology.org) (Ana et al., 2005) and Kyoto Encyclopedia of Genes and Genomes (KEGG) *via* KEGG Automatic Annotation Server (KAAS) (Yuki et al., 2007). GO and KEGG pathway enrichment analyses were applied based on Fisher's exact test. Cluster 3.0 and Java Treeview software were used to construct a heat map and perform hierarchical clustering; while a protein-protein interaction (PPI) network was generated using Cytoscape5 (version 3.2.1) and verified using STRING (http://string-db.org/).

2.14. Quantitative real-time PCR assay

RNA was extracted from *B. microti* treated with either DMSO or 50 μM of 4-NBT by using TRIzol reagent (Invitrogen, Carlsbad, CA, USA). Complementary DNAs (cDNAs) were obtained by using a

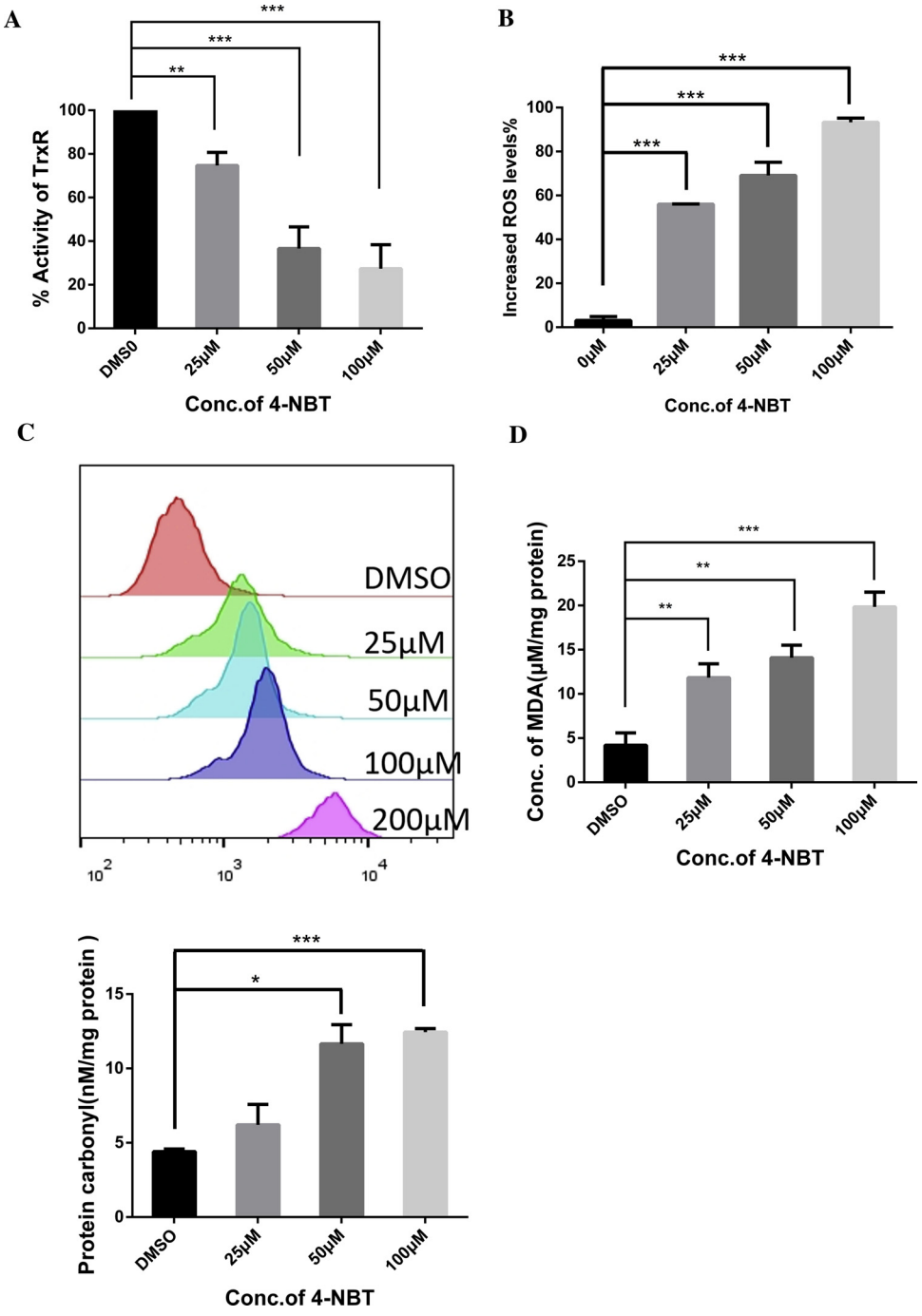

Fig. 2. TrxR activity and the redox state are inhibited by 4-NBT in *B. microti*. (A) TrxR activity was determined using the DTNB reduction method after incubating *B. microti* with different 4-NBT concentrations. Following 4-NBT treatment for 12 h, ROS levels were examined using CellROX® Deep Red reagent staining coupled with flow cytometry. (B) ROS cell percentages and a representative (C) flow cytometric histogram are shown. The effect of 4-NBT on protein carbonyl content was examined spectrophotometrically using (D) DNPH, and lipid peroxidation was determined by measuring (E) MDA. Data are expressed as a mean ± SEM of at least three replicates (n = 3). ***$P < 0.0001$, **$P < 0.001$, and *$P < 0.05$ relative to the DMSO control group, with $P < 0.05$ deemed significant.

PrimeScript™ RT Reagent Kit (Takara, Kusatsu, Japan), and quantitative real-time PCR (qPCR) was performed using TB Green™ Fast qPCR Mix (Takara) according to the manufacturer's instructions. A QuantStudio 5 real-time PCR system (Applied Biosystems, Foster City, CA, USA) was utilized during this experiment, with β-actin used as an internal reference gene. Expression level fold changes were calculated using the $2^{-\Delta\Delta CT}$ method. All of the qPCR amplifications were performed in triplicate and repeated twice, with the mean values considered for comparisons. All of the primers are provided in Supplemental Table 1.

3. Results

3.1. 4-NBT was determined to be a specific B. microti TrxR inhibitor

*Bm*TrxR was obtained *via* recombinant expression, and RTrxR was purchased. DTNB was used as a substrate to measure TrxR activity, with 150 nM of *Bm*TrxR and 50 nM of RTrxR utilized. Each TrxR showed a good inhibitory behavior, with the inhibitory effect increasing in relation to a concentration within a specific range (Fig. 1). Auranofin and CDNB more specifically targeted RTrxR, and Auranofin completely inhibited TrxR within a low nanomolar range. 2,4-DNPS (RTrxR IC_{50} = 427.5 nM, *Bm*TrxR IC_{50} = 560.4 nM) showed a high degree of inhibition, but low selectivity. In contrast, 4-NBT (RTrxR IC_{50} = 50.8 μM, *Bm*TrxR IC_{50} = 11.7 μM) was selective for *Bm*TrxR, with an RTrxR/*Bm*TrxR selectivity value that reached 4.3. Thus, 4-NBT was selected for further experimentation.

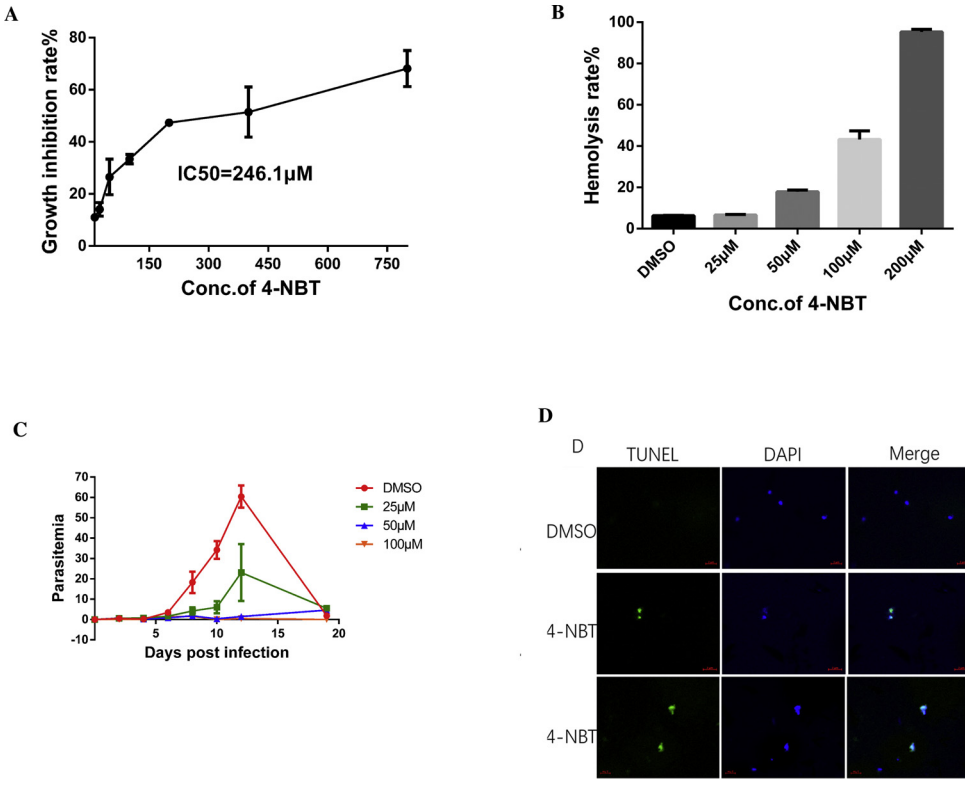

Fig. 3. Effect of 4-NBT on *B. microti* growth and erythrocyte lysis. (A) Growth curve of treated *B. microti in vitro* using the SYBR method, with IC50 values in the diagram. (B) Growth curve of treated *B. microti in vivo*, with parasitemia counted *via* flow cytometry and microscopically. (C) The degree of hemolysis and (D) TUNEL staining showing *in situ* DNA fragmentation were examined in *B. microti* following 4-NBT treatment.

3.2. Effect of 4-NBT on the antioxidant system and on oxidative stress in *B. microti*

To confirm that 4-NBT can inhibit TrxR activity in *B. microti*, a TrxR activity assay was performed, with DTNB used as the substrate. *B. microti* extract that had been treated with DMSO had a protein activity level of 0.41 ± 0.06 U/mg, which was regarded as 100% enzymatic activity. The 25 μM 4-NBT treatment group showed a 74.71% activity level relative to the control, the 50 μM group showed a 36.59% activity level, and the 100 μM group a showed 27.35% level (Fig. 2A). These results indicate that indeed 4-NBT targets TrxR. TrxR plays an important role in redox balance; thus, ROSs and the index of oxidative stress injury were measured *via* a flow cytometer using SYBR® Green and by marking cells with high ROS levels with CellROX® Deep Red reagent. While no difference was noted between healthy RBC incubated with 4-NBT or DMSO, a significant difference was noted when *B. microti* was incubated with DMSO or 4-NBT. *B. microti* treated with DMSO had especially low ROS levels, while much higher levels were seen in *B. microti* treated with 4-NBT. Since 4-NBT inhibits TrxR (Figs. 2B and 2C), *B. microti* was unable to eliminate ROS in a timely fashion. ROS can directly damage proteins and lipids and can produce stable carbonyl groups and MDA. These results indicate that *B. microti* treatment with 4-NBT, to a certain extent, causes lipid and protein peroxidation (Figs. 2D and E). In conclusion, these findings show that 4-NBT inhibits *B. microti* TrxR activity and disrupts redox homeostasis.

3.3. Cytotoxicity of 4-NBT

To further characterize 4-NBT *B. microti*, IC50 was established and found to be 246.1 μM using the SYBR method (Fig. 3A). To further evaluate this finding, erythrocytes with a 40% *B. microti* infection were treated with 25, 50, or 100 μM 4-NBT or DMSO (positive control), with healthy erythrocytes treated with the same volume of DMSO as a negative control. The results showed that the percentages of parasitized cells were similar, but the degree of hemolysis varied among the groups. After 12 h, mice were inoculated with 1×10^8 cells from each group, and the *B. microti* treated with DMSO multiplied the fastest, while those treated with 50 μM or 100 μM replicated at very low levels (Fig. 3C). These results show that *B. microti* treated with DMSO has the highest vitality and infectivity, while those treated with 4-NBT show stunted growth. Additionally, erythrotoxicity was evaluated based on the degree of hemolysis, with 100 μM 4-NBT causing > 40% hemolysis, 50 μM causing ˜20% hemolysis, and 25 μM causing ˜10% hemolysis, which was comparable to the DMSO group (Fig. 3B).

ROS is one of the factors that induce apoptosis and cause oxidative damage. Single-celled protozoan parasites, such as *P. falciparum*, have been shown to induce apoptosis (Mutai and Waitumbi, 2010); thus, a TUNEL assay was performed to examine if this also occurs in *B. microti* infections. In Fig. 3D, the 4-NBT treatments (blue and green dots) were colocalized, thus indicating that the genomic DNA broke and cells were in the later stage of apoptosis, while in contrast, *B. microti* treated with DMSO showed few signs of apoptosis. Ultimately, a concentration of 50 μM was selected for subsequent experimentation.

3.4. Proteomic analysis

B. microti possesses approximately 3500 proteins, which makes it the smallest protozoon in Apicomplexa (Cornillot et al., 2013). Herein, 960 proteins were identified within all the samples (Supplemental file 1), with 118 proteins significantly up-regulated in the TNB group (50 μM 4-NBT) relative to the control and 37 down-regulated (Supplemental file. 2). Differences in the 67 significantly differential proteins that met all of the above criteria were then further examined using clustering (Fig. 4).

Following GO and KEGG analyses, the identified proteins were mainly enriched in the areas of binding, catalytic activity, structural molecule activity, molecular function regulator, and signal transducer activity. Furthermore, GO analysis for biological process (BP), molecular function (MF), and cellular component (CC) of the identified proteins were shown in Fig. 5. Rich factor (≤1) were shown as numbers above the orange bar, which represented the enrichment. And p values (≤0.05) were shown as the orange bar, which represented the

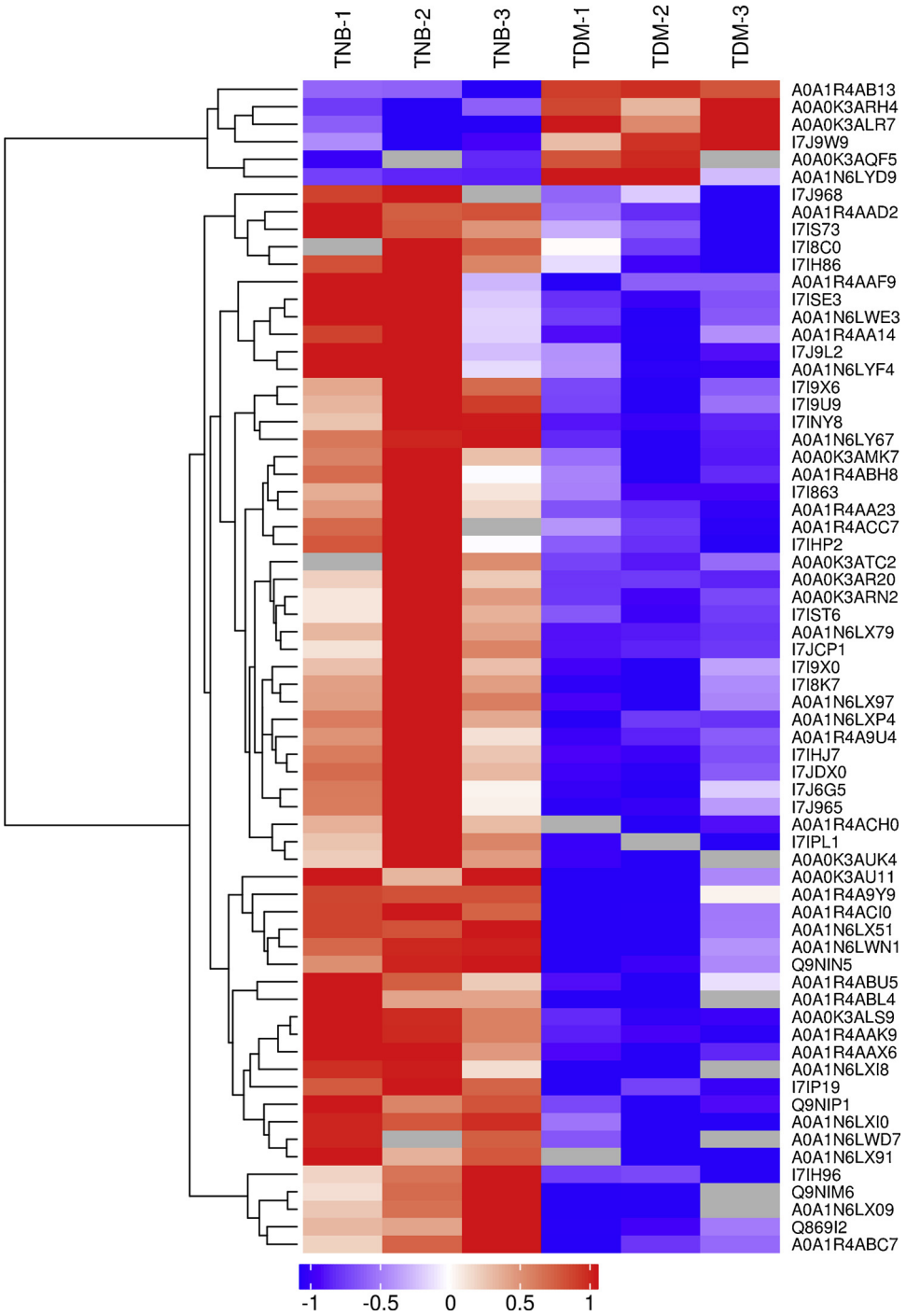

Fig. 4. Heatmap of differentially expressed proteins between TNB (4-NBT-exposed) and TDM (DMSO-exposed) following clustering analysis. A total of 67 differentially expressed proteins in the TNB group relative to TDM were examined. The ratio of protein expression levels between TNB and TDM was standardized, with differential proteins having a ratio > 2 or < 0.5 and *P*-value < 0.05. All sequence hits for quantitative proteins were identified using the UniProtKB database.

significance of enrichment in this GO term. In the biological processes category, the identified proteins were predominantly enriched in the areas of cellular process, metabolic process, biological regulation, regulation of biological process, cellular component organization, and biogenesis. KEGG pathway analysis showed that the identified proteins were predominantly enriched in pathways associated with protein synthesis, processing, and degradation (Fig. 6).

When attempting to quantify the TrxR target protein using MS, levels were undetectable. However, when utilizing Western blotting (Supplemental Fig. 1), a low level of detection was obtained, which was unquantifiable and thus unusable for comparative analysis between the 4-NBT and DMSO groups due to the lack of an internal reference. In the 4-NBT group, Trx1 (A0A286LPJ8), a downstream TrxR target, was identified. Additionally, ribonucleoside-diphosphate reductase (rNDP; A0A1N6LXI8), which has a reducing ability and drives the free radical mechanism of TrxR, had a 14.7-fold increase.

As an Apicomplexan, the metabolic demands of *B. microti* are minimal and highly dependent on glucose fermentation for energy production and redox regulation. In our report, glyceraldehyde-3-phosphate dehydrogenase (GAPDH; *P*-value = 0.0055, fold- change: 7.78) and pyruvate kinase (PK; only detected in TNB) were up-regulated. In glycolysis, PK catalyzes the final step that yields one molecule

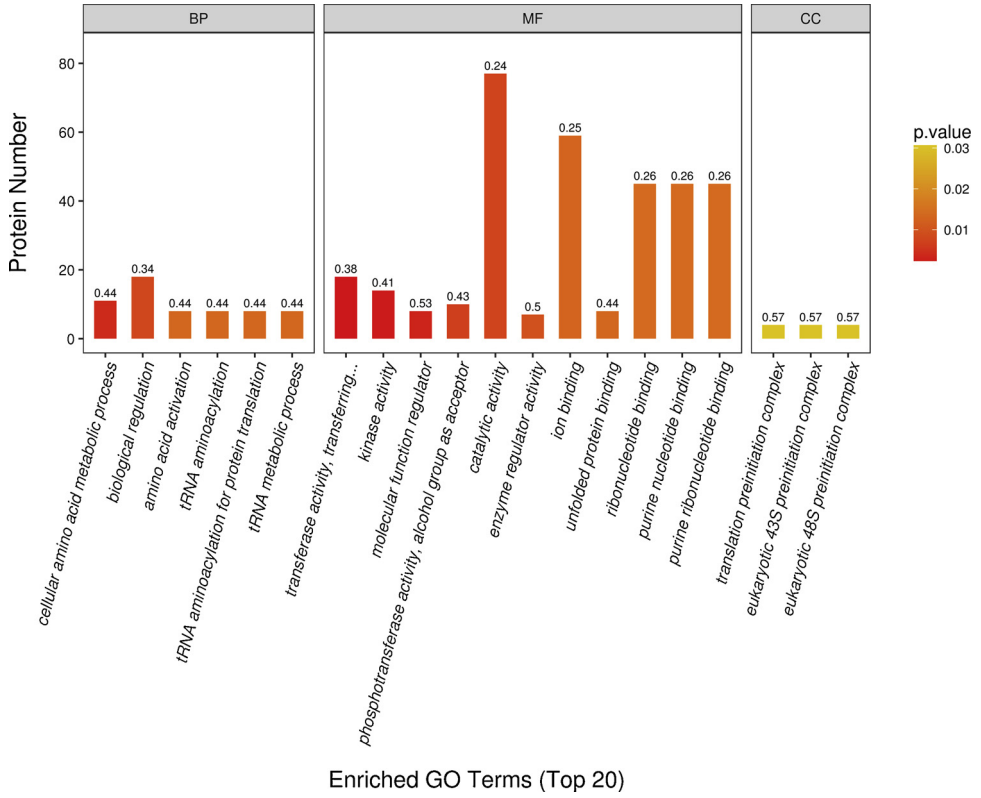

Fig. 5. GO analysis for biological process, molecular function, and cellular component of the identified differential proteins in the TNB group relative to the TDM group.

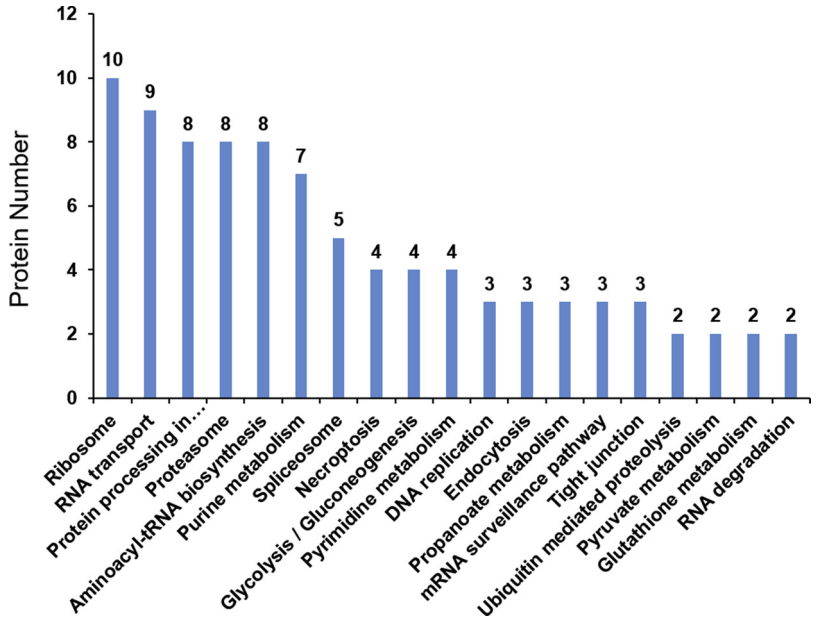

Fig. 6. The top 20 KEGG pathways containing differential proteins in TNB relative to TDM.

of ATP, while GAPDH catalyzes the sixth step and simultaneously reduces NAD^+ to NADH, which can aid cells under oxidative stress. Additionally, GAPDH has been implicated in initiating apoptosis (Tarze et al., 2007) and can act as a chaperone protein for labile heme within cells in the context of maintaining cellular iron homeostasis (Sweeny et al., 2018). Taken together, these findings suggest that ROS is generated following the inactivation of GAPDH and PK in treated *B. microti*, and to gain enough energy and reducing power, namely, ATP and NADH, the organism must then actively attempt to up-regulate GAPDH and PK.

Based on the obtained proteomics results, we selected some differentially expressed and interested proteins and further verified *via* qPCR (Fig. 7). While most of the expression levels were consistent with the MS results, rNDP translation and transcription were not consistent, with protein levels up-regulated when compared to the mRNA levels.

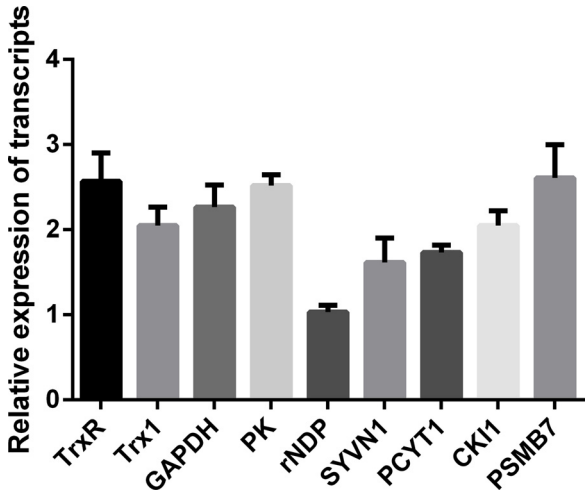

Fig. 7. Relative mRNA expression levels of a subset of nine differential genes examined using qPCR. For each sample, the acquired cycle threshold (CT) was normalized to the CT of the internal housekeeping gene actin, and ΔCT was then normalized to ΔCT of the TNB group. Relative fold differences in mRNA expression levels were calculated using the $2^{-\Delta\Delta CT}$ method. Data are displayed as a mean ± SD of three independent replicates. *$P < 0.05$ indicates a significant difference between group; ns, no significant difference.

4. Discussion

Since *B. microti* is an intraerythrocytic protozoal parasite, identifying a selective *Bm*TrxR inhibitor was necessary. Once 4-NBT was found to specifically inhibit *Bm*TrxR, factors associated with oxidative stress, such as ROS levels, lipid peroxidation, and protein carbonyls, were evaluated. Furthermore, label-free quantitative proteomics was utilized to study the effect of TrxR inhibition on *B. microti* protein expression. The results showed a significant change in expression associated with glycolysis, synthesis, and protein degradation. To our knowledge, this is the first proteomic report to examine *B. microti* without TrxR activity and shows the significance of TrxR in *B. microti* survival.

While Auranofin and CDNB have been shown to be highly efficient in reducing TrxR activity in *P. falciparum* (Andricopulo et al., 2006), 4-NBT (*Pf*TrxR IC_{50} = 2 μM, human TrxR IC_{50} = 50 μm) and 2,4-DNPS (*Pf*TrxR IC_{50} = 0.5 μM, human TrxR IC_{50} = 4 μM) were shown to have the highest specificity of the 15 examined inhibitors. Furthermore, these two inhibitors were found to be noncompetitive and to not significantly interact with the TrxR C-terminal redox center or NADPH binding site. Furthermore, from the report of Andricopulo, 4-NBT (IC50 = 11 μM) showed a good efficiency to anti *plasmodium falciparum* using the detection method of SYBR GREEN I. However, 4-NBT (IC50 = 246.1 μM) showed a poor efficiency to anti *B. microti*. There was not great dissimilarity of TrxR inhibitor effectiveness between *B. microti* and *P. falciparum*, but anti-parasites were huge. What's more, from the results of TUNEL and reinjected perspective, 4-NBT indeed damaged *B. microti*. The SYBR Green I result was doubted, which may be attributed to the culturing method. The technology of *B. microti* culture *in vitro* is still a big problem in the world. And this culture method keeps the parasites in a good state from the view of morphology and the increased number of parasites in single RBC, but the parasitemia cannot rise obviously. Another possible explanation may be that *B. microti* may be dead after 4-NBT treatment, but the DNA still binds the SYBR Green I. Moreover, the TUNEL assay results showed that 4-NBT treatment in *B. microti* promotes apoptosis.

In this study, a label-free technology based on a MaxQuant algorithm for protein quantification was used to identify and analyze the composition and changes in *B. microti* protein expression following 4-NBT treatment relative to DMSO. This is the second study to derive a *B. microti* protein expression profile, with the first study utilizing hydrogel affinity nanoparticles and identifying ~500 proteins (Magni et al., 2018). Herein, 960 proteins were detected, which is nearly double the previous amount and suggests that label-free technology can provide higher sensitivity.

ROS can react directly with cellular lipids, proteins and DNA (Regner et al., 2014) and cause cellular oxidative damage and dysfunction. In this case, *B. microti* would need to repair the DNA, but these markers have yet to be identified. Even still, some up-regulated proteins involved in DNA synthesis and repair, such as A0A1N6LXI8, A0A0K3AQ96, and I7IT34, were identified; with rNDP being a key regulatory enzyme that modulates the rate of DNA synthesis so that the DNA to cell mass is maintained at a constant ratio during cell division and DNA repair(Herrick and Sclavi, 2007).

In lipid metabolism, membrane lipids are the most vulnerable to ROS and have the biggest impact on *B. microti* survival. Choline-phosphate cytidylyltransferase (PCYT1, A0A1N6LX56) was identified only in treated *B. microti* and plays an important role in regulating membrane phosphatidylcholine content. Furthermore, choline/ethanolamine kinase (CKI1, A0A1N6LWH6), which was also up-regulated in 4-NBT treated samples, is an enzyme that catalyzes the first reaction in the choline and ethanolamine pathway for glycerophosphocholine and glycerophosphoethanolamine biosynthesis, which are major membrane phospholipids (Gibellini et al., 2008). Ethanolamine is also a component of the glycosylphosphatidylinositol (GPI) anchor, which is necessary for cell-surface protein attachment (Tian et al., 2006). Long chain acyl-CoA synthetase 5 (A0A1R4A9U4; *P*-value = 0.0327, fold-change = 5.9) was also identified and plays a key role in lipid biosynthesis and fatty acid degradation.

In pathways associated with protein processing in the endoplasmic reticulum, eight differentially expressed proteins were identified. These include disulfide-isomerase A6 (A0A1R4ACL8) (Gruber et al., 2006) and three kinds of heat shock proteins (I7IHJ7, A0A0K3AMK7, and A0A1R4ACI0) (Picard, 2002) that participate in protein folding, E3 ubiquitin-protein ligase synoviolin (SYVN1, A0A1R4ABB7) that participates in protein degradation and unfolding (Lilley and Ploegh, 2005), and others (I7I9 × 0, I7JAC4, A0A1R4ACH6) that play a role in ubiquitination (Lass et al., 2008; Meyer et al., 2000; Zhong et al., 2009). The up-regulation of these proteins suggests that the endoplasmic reticulum is under stress, which correlates with the oxidative stress that is caused by TrxR inhibition. Moreover, dysfunction of the endoplasmic reticulum would result in misfolded and unfolded proteins accumulating. Thus, it should be unsurprising that seven proteasome subunits [A0A1N6LX91, I7J8S2, I7ISS4, I7I8K2, A0A0K3APP5 (PSMB7), A0A0K3ARH8, and A0A1R4AAG6] and nine ribosome subunits (I7IPL1, I7IP19, I7I8K7, I7J968, I7IS73, I7J653, I7JDE2, I7I9Z7, and I7IFK2) were up-regulated to boost protein levels and aid in *B. microti* survival in the presence of 4-NBT

Conflicts of interest

The authors declare no conflict of interest.

Acknowledgement

Project support was provided by the “National Key Basic Research Program (973 program) of China” (Grant No. 2015CB150300).

Appendix A. Supplementary data

Supplementary material related to this article can be found, in the online version, at doi:https://doi.org/10.1016/j.ttbdis.2019.05.004.

References

Ana, C., Stefan, G.T., Juan Miguel, G.G., Javier, T., Manuel, T., Montserrat, R., 2005.

Blast2GO: a universal tool for annotation, visualization and analysis in functional genomics research. Bioinformatics 21, 3674–3676.
Andricopulo, A.D., Akoachere, M.B., Krogh, R., Nickel, C., McLeish, M.J., Kenyon, G.L., Arscott, L.D., Williams Jr, C.H., Davioud-Charvet, E., Becker, K., 2006. Specific inhibitors of *Plasmodium falciparum* thioredoxin reductase as potential antimalarial agents. Bioorg. Med. Chem. Lett. 16, 2283–2292. https://doi.org/10.1016/j.bmcl.2006.01.027.
Bullard, K.M., Broccardo, C., Keenan, S.M., 2015. Effects of cyclin-dependent kinase inhibitor Purvalanol B application on protein expression and developmental progression in intra-erythrocytic *Plasmodium falciparum* parasites. Malar. J. 14, 147. https://doi.org/10.1186/s12936-015-0655-x.
Cornillot, E., Dassouli, A., Garg, A., Pachikara, N., Randazzo, S., Depoix, D., Carcy, B., Delbecq, S., Frutos, R., Silva, J.C., Sutton, R., Krause, P.J., Mamoun, C.B., 2013. Whole genome mapping and re-organization of the nuclear and mitochondrial genomes of *Babesia microti* isolates. PLoS One 8, e72657. https://doi.org/10.1371/journal.pone.0072657.
Cornillot, E., Hadj-Kaddour, K., Dassouli, A., Noel, B., Ranwez, V., Vacherie, B., Augagneur, Y., Bres, V., Duclos, A., Randazzo, S., Carcy, B., Debierre-Grockiego, F., Delbecq, S., Moubri-Menage, K., Shams-Eldin, H., Usmani-Brown, S., Bringaud, F., Wincker, P., Vivares, C.P., Schwarz, R.T., Schetters, T.P., Krause, P.J., Gorenflot, A., Berry, V., Barbe, V., Ben Mamoun, C., 2012. Sequencing of the smallest Apicomplexan genome from the human pathogen Babesia microti. Nucleic Acids Res. 40, 9102–9114. https://doi.org/10.1093/nar/gks700.
Cox, J., Mann, M., 2008. MaxQuant enables high peptide identification rates, individualized p.p.b.-Range mass accuracies and proteome-wide protein quantification. Nat. Biotechnol. 26, 1367–1372. https://doi.org/10.1038/nbt.1511.
Erp, E.E., Smith, R.D., Ristic, M., Osorno, B.M., 1980. Continuous in vitro cultivation of Babesia bovis. Am. J. Vet. Res. 41, 1141–1142.
Gibellini, F., Hunter, W.N., Smith, T.K., 2008. Biochemical characterization of the initial steps of the Kennedy pathway in *Trypanosoma brucei*: the ethanolamine and choline kinases. Biochem. J. 415, 135–144. https://doi.org/10.1042/BJ20080435.
Gruber, C.W., Cemazar, M., Heras, B., Martin, J.L., Craik, D.J., 2006. Protein disulfide isomerase: the structure of oxidative folding. Trends Biochem. Sci. 31, 455–464. https://doi.org/10.1016/j.tibs.2006.06.001.
Herrick, J., Sclavi, B., 2007. Ribonucleotide reductase and the regulation of DNA replication: an old story and an ancient heritage. Mol. Microbiol. 63, 22–34. https://doi.org/10.1111/j.1365-2958.2006.05493.x.
Jortzik, E., Becker, K., 2012. Thioredoxin and glutathione systems in Plasmodium falciparum. Int. J. Med. Microbiol. 302, 187–194. https://doi.org/10.1016/j.ijmm.2012.07.007.
Kavishe, R.A., Koenderink, J.B., Alifrangis, M., 2017. Oxidative stress in malaria and artemisinin combination therapy: pros and Cons. FEBS J. 284, 2579–2591. https://doi.org/10.1111/febs.14097.
Kehr, S., Sturm, N., Rahlfs, S., Przyborski, J.M., Becker, K., 2010. Compartmentation of redox metabolism in malaria parasites. PLoS Pathog. 6, e1001242. https://doi.org/10.1371/journal.ppat.1001242.
Krause, P.J., Lepore, T., Sikand, V.K., Gadbaw Jr, J., Burke, G., Telford 3rd, S.R., Brassard, P., Pearl, D., Azlanzadeh, J., Christianson, D., McGrath, D., Spielman, A., 2000. Atovaquone and azithromycin for the treatment of babesiosis. N. Engl. J. Med. 343, 1454–1458. https://doi.org/10.1056/NEJM200011163432004.
Krnajski, Z., Gilberger, T.W., Walter, R.D., Cowman, A.F., Muller, S., 2002. Thioredoxin reductase is essential for the survival of *Plasmodium falciparum* erythrocytic stages. J. Biol. Chem. 277, 25970–25975. https://doi.org/10.1074/jbc.M203539200.
Lass, A., McConnell, E., Fleck, K., Palamarchuk, A., Wojcik, C., 2008. Analysis of Npl4 deletion mutants in mammalian cells unravels new Ufd1-interacting motifs and suggests a regulatory role of Npl4 in ERAD. Exp. Cell Res. 314, 2715–2723. https://doi.org/10.1016/j.yexcr.2008.06.008.
Levy, M.G., Ristic, M., 1980. *Babesia bovis*: continuous cultivation in a microaerophilous stationary phase culture. Science 207, 1218–1220.
Lilley, B.N., Ploegh, H.L., 2005. Multiprotein complexes that link dislocation, ubiquitination, and extraction of misfolded proteins from the endoplasmic reticulum membrane. Proc. Natl. Acad. Sci. U. S. A. 102, 14296–14301.
Magni, R., Luchini, A., Liotta, L., Molestina, R.E., 2018. Analysis of the *Babesia microti* proteome in infected red blood cells by a combination of nanotechnology and mass spectrometry. Int. J. Parasitol. https://doi.org/10.1016/j.ijpara.2018.08.004.
Meyer, H.A., Grau, H., Kraft, R., Kostka, S., Prehn, S., Kalies, K.U., Hartmann, E., 2000. Mammalian Sec61 is associated with Sec62 and Sec63. J. Biol. Chem. 275, 14550–14557.
Müller, S., 2010. Redox and antioxidant systems of the malaria parasite *Plasmodium falciparum*. Mol. Microbiol. 53, 1291–1305.
Mutai, B.K., Waitumbi, J.N., 2010. Apoptosis stalks *Plasmodium falciparum* maintained in continuous culture condition. Malar. J. 9 (Suppl 3), S6. https://doi.org/10.1186/1475-2875-9-S3-S6.
Nilsson Bark, S.K., Ahmad, R., Dantzler, K., Lukens, A.K., De Niz, M., Szucs, M.J., Jin, X., Cotton, J., Hoffmann, D., Bric-Furlong, E., Oomen, R., Parrington, M., Milner, D., Neafsey, D.E., Carr, S.A., Wirth, D.F., Marti, M., 2018. Quantitative proteomic profiling reveals novel *Plasmodium falciparum* surface antigens and possible vaccine candidates. Mol. Cell Proteomics 17, 43–60. https://doi.org/10.1074/mcp.RA117.000076.
Picard, D., 2002. Heat-shock protein 90, a chaperone for folding and regulation. Cell. Mol. Life Sci. 59, 1640–1648.
Regner, E.L., Thompson, C.S., Iglesias, A.A., Guerrero, S.A., Arias, D.G., 2014. Biochemical characterization of thioredoxin reductase from *Babesia bovis*. Biochimie 99, 44–53. https://doi.org/10.1016/j.biochi.2013.11.002.
Sannella, A.R., Casini, A., Gabbiani, C., Messori, L., Bilia, A.R., Vincieri, F.F., Majori, G., Severini, C., 2008. New uses for old drugs. Auranofin, a clinically established antiarthritic metallodrug, exhibits potent antimalarial effects in vitro: mechanistic and pharmacological implications. FEBS Lett. 582, 844–847. https://doi.org/10.1016/j.febslet.2008.02.028.
Smilkstein, M., Sriwilaijaroen, N., Kelly, J.X., Wilairat, P., Riscoe, M., 2004. Simple and inexpensive fluorescence-based technique for high-throughput antimalarial drug screening. Antimicrob. Agents Chemother. 48, 1803–1806.
Sweeny, E.A., Singh, A.B., Chakravarti, R., Martinezguzman, O., Saini, A., Haque, M.M., Garee, G., Dans, P.D., Hannibal, L., Reddi, A.R., 2018. Glyceraldehyde 3-phosphate dehydrogenase is a chaperone that allocates labile heme in cells. J. Biol. Chem.:jbc.RA 118, 004169.
Tarze, A., Deniaud, A., Le Bras, M., Maillier, E., Molle, D., Larochette, N., Zamzami, N., Jan, G., Kroemer, G., Brenner, C., 2007. GAPDH, a novel regulator of the pro-apoptotic mitochondrial membrane permeabilization. Oncogene 26, 2606–2620. https://doi.org/10.1038/sj.onc.1210074.
Taylor, A.E.R., Baker, J.R., 1987. Vitro Methods for Parasite Cultivation. Academic.
Tian, Y., Jackson, P., Gunter, C., Wang, J., Rock, C.O., Jackowski, S., 2006. Placental thrombosis and spontaneous fetal death in mice deficient in ethanolamine kinase 2. J. Biol. Chem. 281, 28438–28449. https://doi.org/10.1074/jbc.M605861200.
Trager, W., Jensen, J.B., 2005. Human malaria parasites in continuous culture. 1976. J. Parasitol. 91, 484–486. https://doi.org/10.1645/0022-3395(2005)091[0484:HMPICC]2.0.CO;2.
Vannier, E., Gewurz, B.E., Krause, P.J., 2008. Human babesiosis. Infect. Dis. Clin. North Am. 22, 469–488. https://doi.org/10.1016/j.idc.2008.03.010. viii-ix.
Vannier, E., Krause, P.J., 2012. Human babesiosis. N. Engl. J. Med. 366, 2397–2407. https://doi.org/10.1056/NEJMra1202018.
Wisniewski, J., Zougman, A., Nagaraj, N., Mann, M., 2009. Universal sample preparation method for proteome analysis. Nat. Methods 6, 359–362.
Yuki, M., Masumi, I., Shujiro, O., Yoshizawa, A.C., Minoru, K., 2007. KAAS: an automatic genome annotation and pathway reconstruction server. Nucleic Acids Res. 35, 182–185.
Zhang, H., Wang, Z., Gong, H., Cao, J., Zhou, Y., Zhou, J., 2016. Identification and functional study of a novel 2-cys peroxiredoxin (BmTPx-1) of Babesia microti. Exp. Parasitol. 170, 21–27. https://doi.org/10.1016/j.exppara.2016.08.005.
Zhao, S., Gong, H., Zhou, Y., Zhang, H., Cao, J., Zhou, J., 2016. Identification of a thioredoxin reductase from *Babesia microti* during mammalian infection. Parasitol. Res. 115, 3219–3227. https://doi.org/10.1007/s00436-016-5084-4.
Zhong, B., Zhang, L., Lei, C., Li, Y., Mao, A.P., Yang, Y., Wang, Y.Y., Zhang, X.L., Shu, H.B., 2009. The ubiquitin ligase RNF5 regulates antiviral responses by mediating degradation of the adaptor protein MITA. Immunity 30, 397–407. https://doi.org/10.1016/j.immuni.2009.01.008.